

# Application of Special Waveform Signals for Eddy Current Testing of Materials

V.V. Polyakov<sup>a)</sup>, Ya.J. Gracheva<sup>b)</sup>, A.V. Egorov<sup>c)</sup>, and A.A. Lependin<sup>d)</sup>

*Altai State University, 61, Lenina pr., Barnaul, 656049, Russia*

<sup>a)</sup>Corresponding author: [pvv@asu.ru](mailto:pvv@asu.ru), <sup>b)</sup> [server2791@mail.ru](mailto:server2791@mail.ru), <sup>c)</sup> [egav@bk.ru](mailto:egav@bk.ru), <sup>d)</sup> [andrey.lependin@gmail.com](mailto:andrey.lependin@gmail.com)

**Abstract.** In this paper, an approach for multi-frequency eddy current testing based on special waveform excitation signals is presented. Digital processing of received signals provides the data for experimental hodographs of a “sensor – testing sample” system. Hodographs for testing samples of aluminum materials with applied dielectric layer demonstrates the reliability of the proposed approach. Application of principal component analysis improves testing parameters identification and differentiation. Obtained results can be used in systems for nondestructive testing of metallic materials and products.

## INTRODUCTION

Eddy current testing is one of the well-known and popular methods for testing metallic materials. It is quite difficult to single out a testing parameter from all influencing factors when the testing is done using a single-frequency excitation signal. A multi-frequency approach producing a hodograph of a “sensor – testing sample” system claims to be more robust and effective [1-3]. The experimental hodograph reveals the combined influence of all factors essential to the eddy current testing. However, there is a shortcoming in the multi-frequency approach: a sequential use of frequencies in a wide range is required [4]. This results in proliferation of a number of measurements and increase of testing time. In this paper, a single-measurement approach to produce a hodograph is proposed. For this single measurement, a sensor is excited by a special waveform signal combined of all set of signals with frequencies from the required range. The proposed approach is tested on aluminum samples of various thicknesses with applied dielectric layer. Projection methods of multivariate data analysis are used for measurement results processing to ensure the reliability of the testing [5-7].

## 1. MEASURING EQUIPMENT

All measurements are performed in automated mode, and parameters at different frequencies are obtained simultaneously. A simplified scheme of the automated measuring and computing complex is shown in Fig.1. The PC with a control program 1 is used to create a data array of instantaneous values of excitation eddy currents. Then, the signal  $u_1(t)$  is synthesized from the data array values and sent to the PC sound card 2 output. A measuring circuit combined with the parametric sensor 3 (where  $L$  – is inductance, and  $r$  – is coil resistance) and the calibration resistor  $R$  is connected to the PC sound card inputs and the output. Time-based measurements of input  $u_1(t)$  and output  $u_2(t)$  signals are performed by analog-digital converters of the PC sound card. Data arrays of input  $\{u_n^{(1)}\}$  and output  $\{u_n^{(2)}\}$  signals are processed then by the control program.

The relation between input  $u_1(t)$  and output  $u_2(t)$  signals is described by the differential equation (1):

$$\frac{du_2}{dt} + \frac{R+r}{L}u_2 = \frac{R}{L}u_1. \quad (1)$$

Fourier transformations of the signals ( $\hat{U}_1$  and  $\hat{U}_2$  respectively) are connected by the relation:

$$\hat{U}_2 = \hat{K}(j\omega)\hat{U}_1, \quad (2)$$

where  $\hat{K}(j\omega)$  - is the complex transfer coefficient of measuring circuit at frequency  $\omega_m$  ( $j = \sqrt{-1}$ ). The  $\hat{K}(j\omega)$  parameter is calculated as follows:

$$\hat{K}(j\omega) = \frac{R}{R+r+j\omega L}. \quad (3)$$

A ferrite coil with a half-shell core is used as an attachable parametric sensor. The core has its magnetic conductivity 2000, and its diameter is 20 mm. A copper-wired coil is placed inside the core. The calibration resistor  $R = 50 \text{ Ohm}$ .

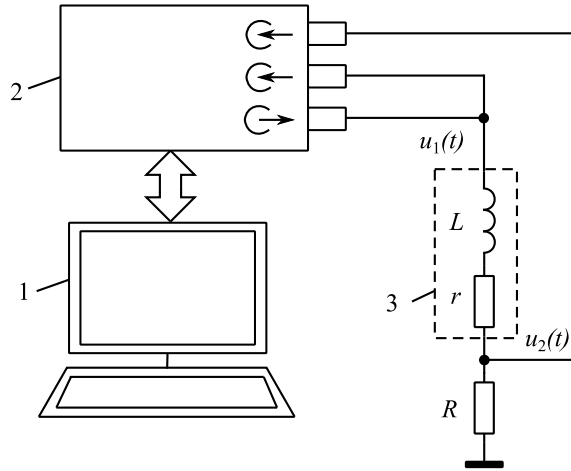


**Figure 1.** A simplified scheme of the automated measuring and computing complex for multifrequency eddy current testing.

## 2. EXPERIMENTAL APPROACH

A signal  $u_1(t)$  composed of  $M$  harmonic signals with frequencies  $\omega_1, \dots, \omega_M$  is transmitted to the input of the sensor:

$$u_1(t) = u_0 \sum_{m=1}^M \sin(\omega_m t), \quad (4)$$

( $u_0$  – is a normalizing constant). An output signal  $u_2(t)$  from the sensor is processed by Fourier transformation, and the Fourier transform  $\hat{U}_2$  of the output signal is calculated as follows:

$$\hat{U}_2 = \sum_{m=1}^M \hat{K}(j\omega_m) \hat{U}_{1m}, \quad (5)$$

where  $\hat{U}_{1m}$  – is the Fourier transform of  $u_1(t)$ ,  $\hat{K}(j\omega)$  – is the complex transfer coefficient of measuring circuit at frequency  $\omega_m$ . According to (5), the output signal spectrum is a line spectrum that contains sensor parameters data at various frequencies. Discrete Fourier transformation is used to analyze the spectrum and to calculate complex amplitudes  $\dot{U}_k^{(1)}$  and  $\dot{U}_k^{(2)}$  of input and output signals [8]:

$$\begin{cases} \dot{U}_k^{(1)} = \sum_{n=0}^{N-1} u_n^{(1)} e^{-j(\frac{2\pi kn}{N})} \\ \dot{U}_k^{(2)} = \sum_{n=0}^{N-1} u_n^{(2)} e^{-j(\frac{2\pi kn}{N})} \end{cases} \quad (6)$$

Equation (6) is used then to obtain eddy current sensor parameters  $X$  and  $r$  at given frequencies  $\omega_m$  for attempts with and without a testing sample. For every given frequency, changes in reactance  $\Delta X(\omega_m) = X(\omega_m) - X_0(\omega_m)$  and resistance  $\Delta r(\omega_m) = r(\omega_m) - r_0(\omega_m)$  of the sensor are calculated. Here,  $X(\omega_m)$  and  $r(\omega_m)$  – are sensor parameters for the attempt with a testing sample,  $X_0(\omega_m)$  and  $r_0(\omega_m)$  – are sensor parameters for the attempt without a testing sample. Measurements are performed by the automated measuring and computing complex introduced in [3,9]. A ferrite coil is used as an attachable parametric sensor. Experimental hodographs are plotted in coordinates of “ $\Delta X/X_0$ ” versus “ $\Delta r/X_0$ ”.

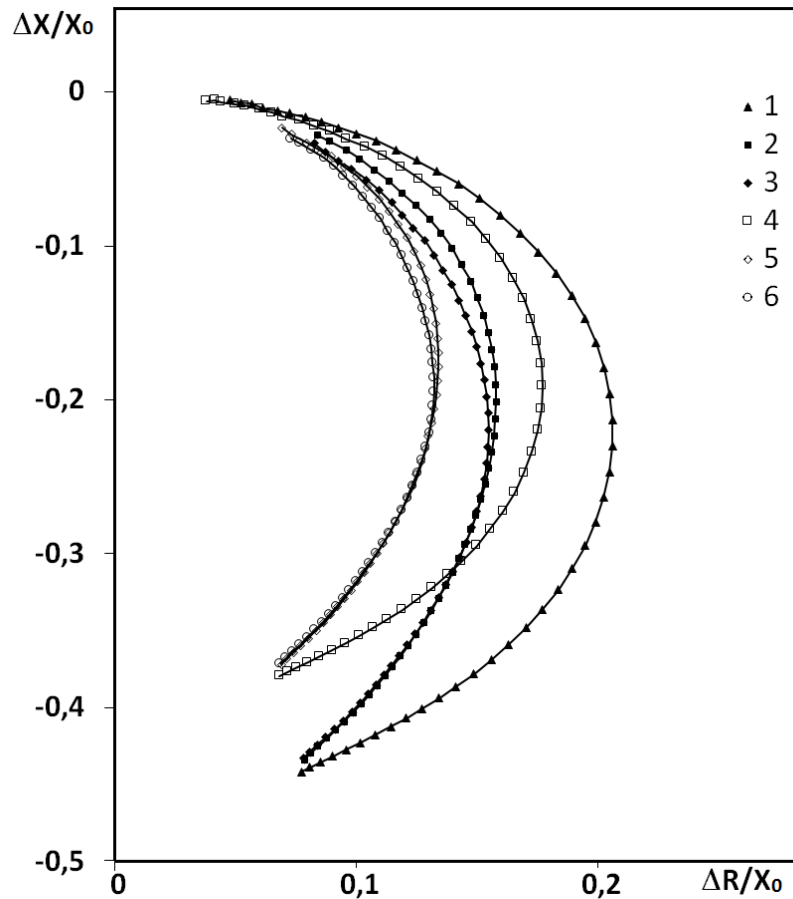


**FIGURE 2.** Experimental hodographs for aluminum samples of various thicknesses with applied dielectric layer. Dielectric layer thickness  $s = 0.6$  mm, plate thickness  $h$ : 1 – 1.43 mm, 2 – 5.72 mm, 3 – 8.61 mm;  $s = 0.2$  mm,  $h$ : 4 – 1.43 mm, 5 – 5.72 mm, 6 – 8.61 mm.

### 3. TESTING SAMPLES AND MEASUREMENTS

Flat aluminum plates of various thicknesses with applied dielectric layer are used as testing samples. This particular choice can be explained by the widely-spread usage of aluminum-based materials in aviation and car industry. Plate thickness  $h$  is varied from 1 mm to 11 mm to guarantee skin effect influence. Dielectric layers are simulated by applying layers of nonconductive materials with predefined thickness. Dielectric layer thickness  $s$  is varied from 0.2 mm to 0.6 mm.

The experimental approach presented earlier is utilized to produce a set of experimental hodographs (Fig.2) for testing samples with different dielectric layer thicknesses (0.2 mm, 0.6 mm) and aluminum plate thicknesses (1.43 mm, 5.72 mm, 8.61 mm). Fig.2 shows the difference along the axis  $\Delta X/X_0$  between hodographs for samples with different thickness  $s$  and the same (constant) thickness  $h$ . It is clearly demonstrated by the lower parts of hodographs that correspond to the high-frequency area. Also, it is revealed that difference of plate thickness  $h$  changes the hodograph form (while thickness  $s$  remains constant). This is most noticeable when values of thickness  $h$  are small. With the increase of  $h$  the difference between hodographs becomes smaller, and, later, hodographs are overlapped. This behavior is explained by the influence of skin layer, especially, when plate thickness is smaller than the skin layer depth. In other cases, when the value of plate thickness  $h$  far exceeds the skin layer depth, the influence of  $h$  is not that strong. This is the natural limitation of capabilities of eddy current testing techniques to inspect thickness of metallic samples.

### 3. APPLICATION OF PRINCIPAL COMPONENT ANALYSIS

Hodographs overlapping shown in Fig.1 demonstrates that simultaneous measurement of plate and dielectric layer thicknesses is quite problematic. Thus, principal component analysis (PCA) is used to process measurement data. Reactance and resistance measurements can be treated as point coordinates in a multidimensional space. Latent dependencies can be revealed by transformation to a new coordinate system to reduce the number of dimensions. Each sample is represented as a single point in the  $2n$ -dimensional space where  $n$  – is the number of frequencies used to plot hodographs. Results of processing are treated as projections on planes of the first and the second principal components PC1 and PC2.

Typical processing results for three different values of plate and dielectric layer thicknesses are presented in Fig.3. Samples with the same values of  $h$  and  $s$  are clustered together. Small differences inside cluster groups are explained by measurement errors. There are several different cluster groups of samples with different  $h$  and the same  $s$  values. They represent different, clearly distinguishable lines on a plane along the first component PC1 axis. When the  $h$  parameter increases, the distance between these clusters becomes smaller and smaller until they overlap each other. This fact also reveals low effectiveness of thickness inspection and differentiation when  $h$  is sufficiently bigger than the skin layer depth. Analysis of Fig.2 demonstrates that application of PCA improves the measurement of thicknesses of aluminum samples with applied dielectric layers.

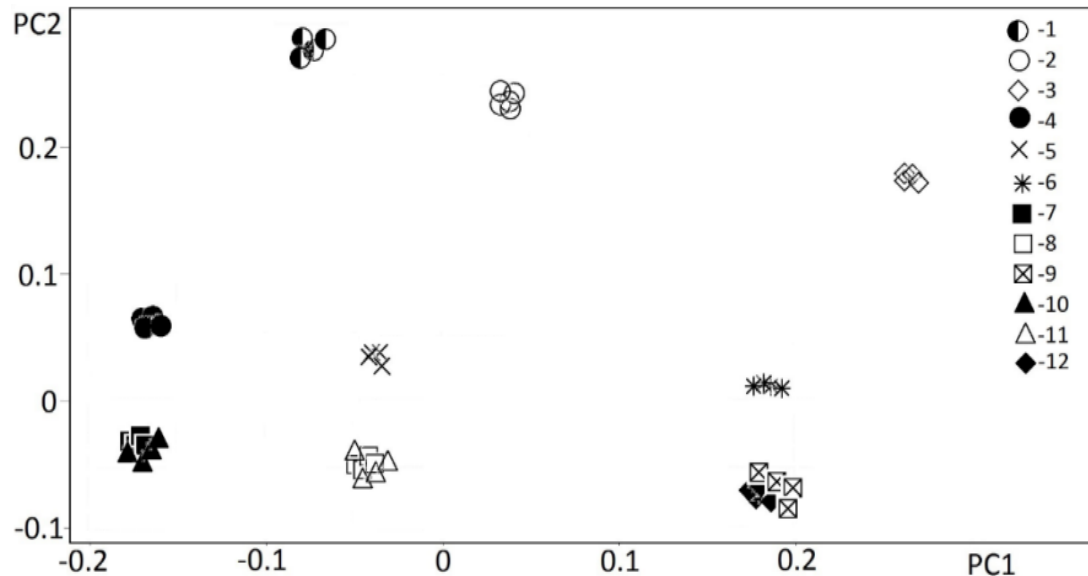


**FIGURE 3.** Projections of experimental data on planes of the first and the second principal components. Dielectric layer thickness  $s = 0$ , plate thickness  $h$ : 1 – 1.43 mm, 4 – 2.85, 7 – 5.72 mm, 10 – 8.61 mm;  $s = 0.2$  mm,  $h$ : 2 – 1.43 mm, 5 – 2.85 mm, 8 – 5.72 mm, 11 – 8.61 mm, 14 – 21.3 mm;  $s = 0.6$  mm,  $h$ : 3 – 1.43 mm, 6 – 2.85 mm, 9 – 5.72 mm, 12 – 8.61 mm.

## CONCLUSION

The proposed approach of multi-frequency eddy current testing based on the application of special waveform signals demonstrates its effectiveness to produce experimental hodographs in a wide range of frequencies. Measurement time is decreased proportionally to the number of frequencies used for measurements. Attained accuracy of hodograph plotting is sufficient to analyze the importance of various testing parameters. Application of PCA for measurement results processing allows improving of testing parameters identification and differentiation. Obtained results significantly enhance eddy current testing capabilities and can be used in various problems of nondestructive testing of metallic materials.

## ACKNOWLEDGMENTS

The work was carried out at the financial support of the RFFI in the framework of the grant №17-08-00914.

## REFERENCES

1. J. García-Martín, J. Gómez-Gil, and E. Vázquez-Sánchez, *Sensors (Basel)* **11**, 2525–2565 (2011).
2. B. Sasi, B.P.C. Rao, Jayakumar, and B. Raj, *Defence Science Journal* **59**, 106-112 (2009).
3. A.V. Egorov, V.V. Polyakov, D.S. Salita, E.A. Kolubaev, S.G. Psakhie, A.G. Chernyavskii, and I.V. Vorobei, *Defence Technology* **11**, 99-103 (2015).
4. L. Lingqi, K. Tsukada, K. Hanasaki, and L. Zheng, *Proceedings of the Fifth International Conference on Information Fusion* **1**, 108-113 (2002).
5. K.H. Esbensen, *Multivariate Data Analysis – In Practice* (CAMO Process AS, Oslo, 2002).
6. S. Shokralla, J.E. Morelli, and T.W. Krause, *IEEE Sens. J.* **16**, 3147–3154 (2016).
7. A.V. Egorov, S.V. Kucheryavskiy, and V.V. Polyakov, *Chemometrics and Intelligent Laboratory Systems* **160**, 8-12 (2017).
8. J. Max, *Methodes es techniques de traitement du signal et applications aux mesures physiques* (Masson, Paris, 1987).
9. V.V. Polyakov, A.V. Egorov, *Russian Journal of Nondestructive Testing* **51**, 631-636 (2015).